APPLICATION OF POSITION-DEPENDENT DELAYED-NEUTRON FRACTIONS TO IQS CALCULATIONS FOR PT-SCWR

Q. Liu[1], E. Nichita[2]
University of Ontario Institute of Technology, Ontario, Canada
[1]Qingjie.Liu@uoit.ca
[2]Eleodor.Nichita@uoit.ca

Abstract

Delayed-neutron fractions depend on fuel burnup and therefore they are position-dependent because fuel burnup is position dependent. This study investigates the use of position-dependent delayed-neutron fractions for Improved Quasistatic kinetics calculations. A new module, MODPARA, is developed and implemented in the 3-D diffusion code DONJON for this purpose. The position dependence of delayed-neutron fractions is taken into account in the calculation of both the amplitude function and the flux shape function during the transient. The amplitude function is primarily influenced by the whole-core effective delayed neutron fractions which are now calculated by accounting for the spatial dependence of the local delayed-neutron fractions. Transient calculations for the Pressure-Tube Super-Critical-Water-cooled Reactor (PT-SCWR) show that accounting for the position dependence of the delayed-neutron fractions changes the time dependence of the amplitude function by as much as 11% compared to the case where position-independent delayed-neutron fractions are used and thus is a desirable enhancement to the IQS method.

1. Introduction

The Improved-Quasi-Static (IQS) method [1, 2] has been widely applied in nuclear reactor space-time kinetics analysis. The key of this method is to factorize the time-space dependent neutron flux into an amplitude function depending solely on time and a shape function dependent on both space and time as in Eq. (1).

$$\Phi_g\left(\vec{r},t\right) = p(t)\Psi_g(\vec{r},t) \tag{1}$$

where $\Phi_g\left(\vec{r},t\right)$ is the space-time group flux, $p(t)$ is the amplitude function, $\Psi_g(\vec{r},t)$ is the shape function.

By inserting Eq. (1) into the space-time neutron- and precursor-balance equations, point kinetics-like equations for the amplitude and precursors are obtained:

$$\begin{aligned}
\dot{p}(t) &= p(t)\frac{\rho(t)-\beta(t)}{\Lambda(t)} + \sum_{k=1}^{k_{\max}} \lambda_k \hat{C}_k(t) \\
\frac{\partial}{\partial t}\hat{C}_k(t) &= p(t)\frac{\beta_k(t)}{\Lambda(t)} - \lambda_k \hat{C}_k(t) \quad (k=1,\ldots,k_{\max})
\end{aligned} \tag{2}$$

The flux shape function can then be shown to satisfy the following equation:

$$
\begin{aligned}
&\frac{dp(t)}{dt}\frac{1}{\bar{v}_g}\Psi_g\left(\vec{r},t\right)+p(t)\frac{\partial}{\partial t}\left[\frac{1}{\bar{v}_g}\Psi_g\left(\vec{r},t\right)\right]=-p(t)\Big\{\nabla\cdot\left[D_g(\vec{r},t)\nabla\Phi_g(\vec{r},t)\right]-\\
&\Sigma_{rg}(\vec{r},t)\Phi_g(\vec{r},t)+\sum_{g'\neq g}\Sigma_{sg'\to g}(\vec{r},t)\Phi_{g'}(\vec{r},t)\Big\}+\\
&p(t)\chi_{pg}(\vec{r},t)[1-\beta(\vec{r},t)]\sum_{g'}\nu\Sigma_{fg'}(\vec{r},t)\Phi_{g'}(\vec{r},t)+\sum_{k=1}^{k_{\max}}\lambda_k\left[\chi_{dkg}(\vec{r},0)C_k(\vec{r},0)e^{-\lambda_k t}+\right.\\
&\left.\int_0^t e^{-\lambda_k(t-t')}p(t')\Psi_g^*(\vec{r})\chi_{dkg}(\vec{r},t')\beta_k(\vec{r},t')\times\sum_{g'}\nu\Sigma_{fg'}(\vec{r},t')\Psi_{g'}(\vec{r},t')\,dt'\right]
\end{aligned}
\tag{3}
$$

Effective kinetics parameters in Eq. (2) (such as β and Λ) for the entire core are calculated as ratio of bilinear functionals of the time-dependent flux shape and steady-state adjoint. By contrast, in Eq. (3), the delayed-neutron fractions are considered position dependent due to the different fuel burnup and hence different fuel properties at different positions.

While proprietary PHWR-core neutronic codes, such as RFSP [3], have been able to account for the position-dependence of delayed-neutron fractions, the IQS module of the 3D diffusion code DONJON [4] has only been able to use space-independent delayed-neutron fractions, assumed to be equal to their effective values for the whole core. The values of the delayed-neutron fractions had to be provided as user input. This work enhances the capabilities of DONJON by allowing the effective delayed-neutron fractions to be represented as position dependent.

2. Position-dependent delayed-neutron fractions in IQS calculations

2.1 Code modification

A new module, MODPARA, is developed, which is capable of accounting for position-dependent delayed-neutron fractions and calculating whole-core effective delayed-neutron fractions for point kinetics and shape function calculation. Whole-core effective delayed-neutron fractions are updated according to the change of flux shape during transient, based on Eq. (4).

$$
\beta_k(t)=\frac{\displaystyle\int_{V_{core}}\left[\sum_g\Psi_g^*(\vec{r})\chi_{dkg}(\vec{r},t)\beta_k(\vec{r},t)\sum_{g'}\nu\Sigma_{fg'}(\vec{r},t)\Psi_{g'}(\vec{r},t)\right]dV}{\displaystyle\int_{V_{core}}\left[\sum_g\Psi_g^*(\vec{r})\chi_g(\vec{r},t)\sum_{g'}\nu\Sigma_{fg'}(\vec{r},t)\Psi_{g'}(\vec{r},t)\right]dV}
\tag{4}
$$

Additionally, the IQS module is modified so that it accounts for the position-dependence of delayed-neutron fractions in Eq. (3).

2.2 PT-SCWR basics

The Pressure-Tube Supercritical-Water Cooled Reactor (PT-SCWR) evolved from the CANDU version of the Pressurized Heavy-Water Reactor (PHWR). It is one of the Gen-IV high-thermal-efficiency concepts [5]. Compared to the regular PHWR, the PT-SCWR presents a more heterogeneous core because of the much higher discharge burnup and greater variation of coolant density. The core consists of a vertical cylindrical vessel containing heavy-water moderator at low temperature and pressure and 336 vertical pressure tubes arranged in a rectangular array, as shown in Fig. 1. Each pressure tube is lined by a ceramic thermal insulator and has a central inner flow tube. The fuel assembly is located between the inner flow tube and the outer ceramic insulator and consists of 62 fuel rods 5m in length, arranged in two concentric annuli. The fuel is a combination of ThO_2 and PuO_2, with Pu representing 15 % by heavy element weight in the inner fuel ring and 12% by heavy-element weight in the outer fuel ring. The initial isotopic composition of Pu is taken to correspond to 44 KWd/kg PWR spent fuel (originally enriched to 4.1%)

The supercritical-water coolant enters the fuel channel at its top and flows downwards through the flow tube and then upwards between the flow tube and the thermal insulator, cooling the fuel assembly in re-entrant pattern. The coolant density decreases substantially from the core bottom (~0.46g/cm^3) to the top (~0.065g/cm^3). The thermal insulator which lines the interior of the pressure tube prevents heat losses to the moderator and thus helps maintain the low temperature and pressure of the moderator.

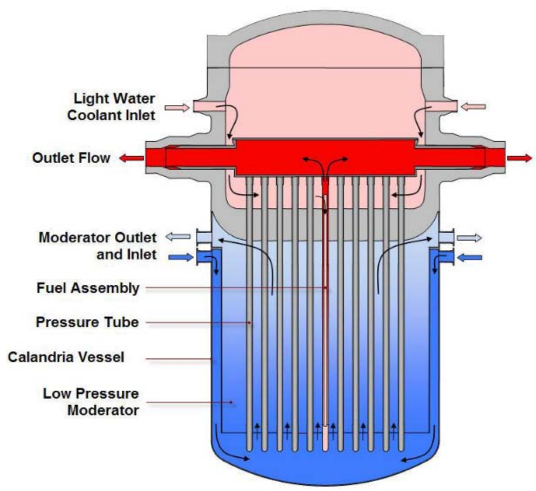

Figure 1 Re-Entrant Channel PT-SCWR Core [5].

2.3 Calculation model

Two-group macroscopic cross sections are generated for the PT-SCWR fuel assembly (Fig. 2) using the lattice code DRAGON [6] which is used to first perform a 69-group collision-probability lattice-level calculation followed by condensation to two groups. The 69-group microscopic cross-sections are obtained from the IAEA-WLUP Library [7].

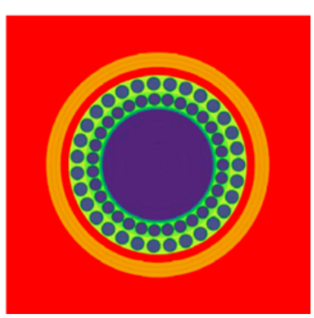

Figure 2 PT-SCWR Lattice-Cell model.

The PT-SCWR utilizes batch refuelling (Fig. 3) with different burnup fuel regions where the effective delayed-neutron fractions differ. Because of the presence of the inner flow tube, a loss of coolant accident scenario will likely see first a voiding of the coolant in the region between the flow tube and the ceramic insulator, the one in direct contact with the fuel, and only later a full voiding of the coolant in the inner flow tube. It is therefore important to understand coolant void reactivity and the transient characteristics during voiding scenario of PT-SCWR. To test the functionality of the newly-developed DONJON module, a coolant-voiding-induced transient is simulated using both position-independent delayed-neutron fractions and position-dependent delayed-neutron fractions. The calculation geometry is shown in Fig. 3. The core is axially divided into 10 regions to account for the change in coolant density [8].

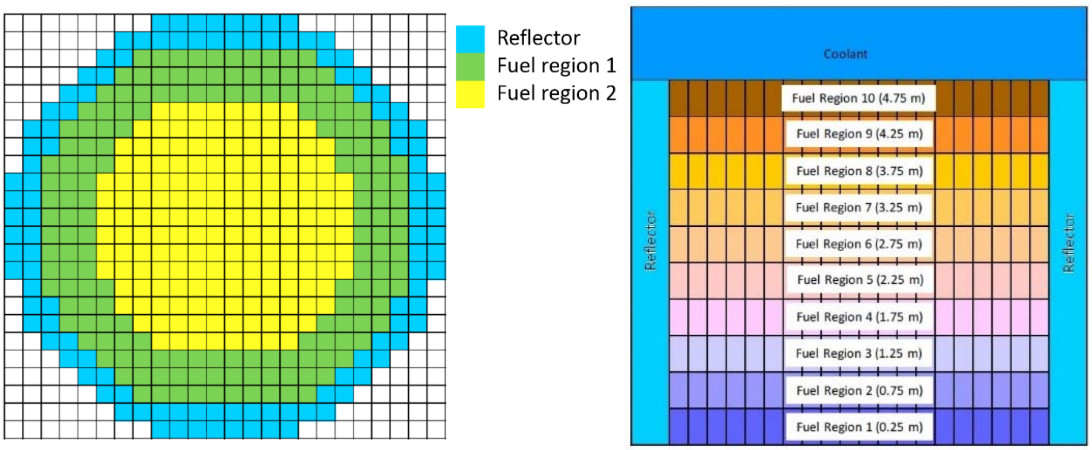

Figure 3 Two batch fuel loading and side view of PT-SCWR Core [8].

3. Calculations and results

The core is initially at steady state loaded with two regions of fuel as shown in Fig. 3 at the burnup of 10MWd/kg and 30MWd/kg. This work uses a loading pattern whereby the inner fuel region has a burnup of 30 MWd/kg. Results are also compared with previous results obtained for a loading pattern characterized by 10 MWd/kg burnup in the inner region [9]. The delayed-neutron fractions corresponding to each burnup are the ones previously determined in Ref. [10]. Kinetics results obtained using both position-dependent and position-independent delayed-neutron fractions are generated and compared for several PT-SCWR transient scenarios.

3.1 Partial voiding scenario

Reactivity insertion is characterized by a partial-core coolant voiding, assumed to occur only in the central fuel region at t=0.0 s. No shutdown-system intervention is simulated. Calculations are performed using position-independent (PI) delayed-neutron fractions as well as position-dependent (PD) ones. The position-independent delayed-neutron fractions are calculated as simple volume averages of the delayed-neutron fractions at the two burnups.

Results in Table 1 show that, while the effective delayed-neutron fractions calculated using the PI model are close to the arithmetic mean of the values for the two fuel regions, the effective delayed-neutron fractions calculated using the PD model are closer to the values in the low burnup fuel region.

Table 1 Effective delayed-neutron fractions.

Delayed-neutron group	Assembly effective β_k 10MWd/kg	30MWd/kg	Whole core effective β_k PI	PD (10MWd/kg fuel in the center)	PD (30MWd/kg fuel in the center)
1	9.55E-05	1.06E-04	1.01E-04	9.58E-05	9.74E-05
2	7.52E-04	7.73E-04	7.63E-04	7.53E-04	7.56E-04
3	5.33E-04	5.48E-04	5.40E-04	5.33E-04	5.36E-04
4	1.15E-03	1.19E-03	1.17E-03	1.15E-03	1.16E-03
5	6.09E-04	6.19E-04	6.14E-04	6.09E-04	6.11E-04
6	2.04E-04	2.09E-04	2.06E-04	2.04E-04	2.05E-04
total	3.34E-03	3.45E-03	3.40E-03	3.35E-03	3.36E-03

Fig. 4 shows the normalized thermal flux shape and thermal adjoint flux distribution in the radial direction for the core mid-plane. Both the flux and the adjoint are higher in the low burnup region, whether low burnup fuel is loaded in the central or the peripheral region of the core. This indicates that the kinetics parameters of the low burnup fuel are always highly weighted. Therefore, swapping the location of low and high burnup fuel has little effect on the whole-core effective delayed-neutron fractions.

Fig. 5 shows the relative core power as a function of time during the partial voiding scenario. The reactivity insertion caused by central region voiding is different for different fuel loading patterns. The larger the reactivity introduced in core, the larger the observed difference between PD and PI results. The difference in relative core power for the two fuel loading patterns is 2.2% and 11%, respectively.

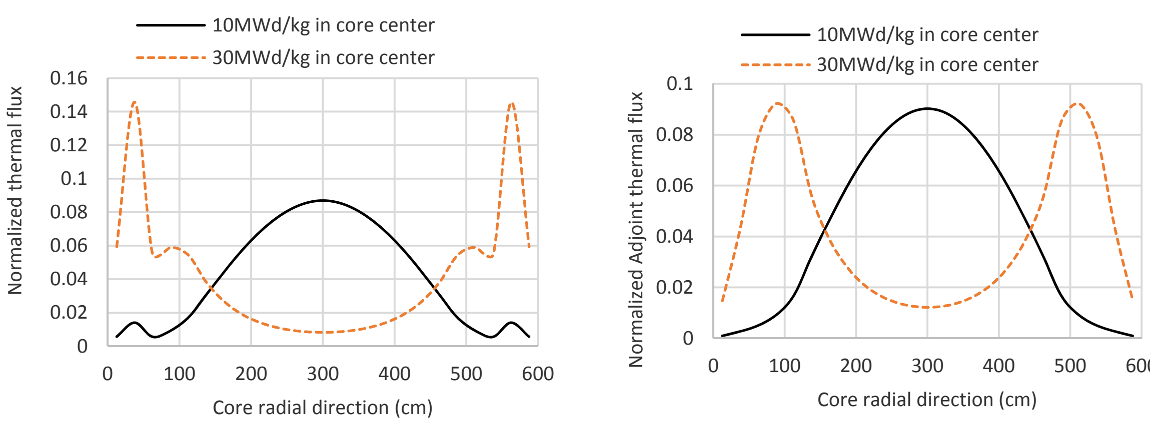

Figure 4 Radial shape of the thermal flux and the thermal adjoint

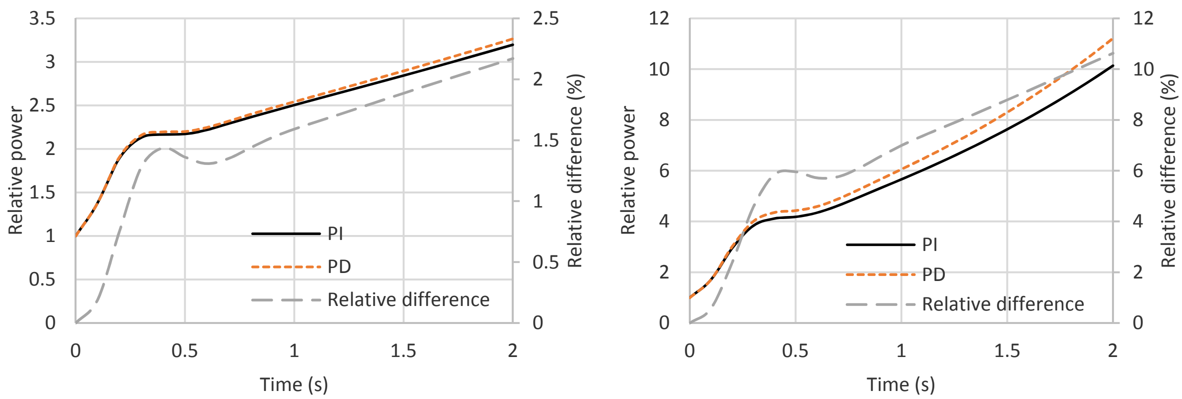

a) 30 MWd/kg fuel in the center b) 10 MWd/kg fuel in the center (reproduced from Ref. [9])

Figure 5 Relative core power as a function of time

3.2 Enhanced reactivity scenario

An enhanced voiding scenario, similar to the one in Ref. [9], was simulated for the 10MWd/kg fuel in-the-centre loading pattern, by increasing the reactivity insertion to 2.96mk, thus bringing the transient closer to prompt criticality.

Fig. 6 shows the core relative power as a function of time for this scenario. It can be seen that the power increases rapidly and the difference in the core relative power between the PD and the PI models also increases up to 280% at 2.0s. It can be inferred from Eq. (2) that when reactivity is closer to prompt criticality, small differences in the delayed-neutron fractions can bring about significant differences in core power.

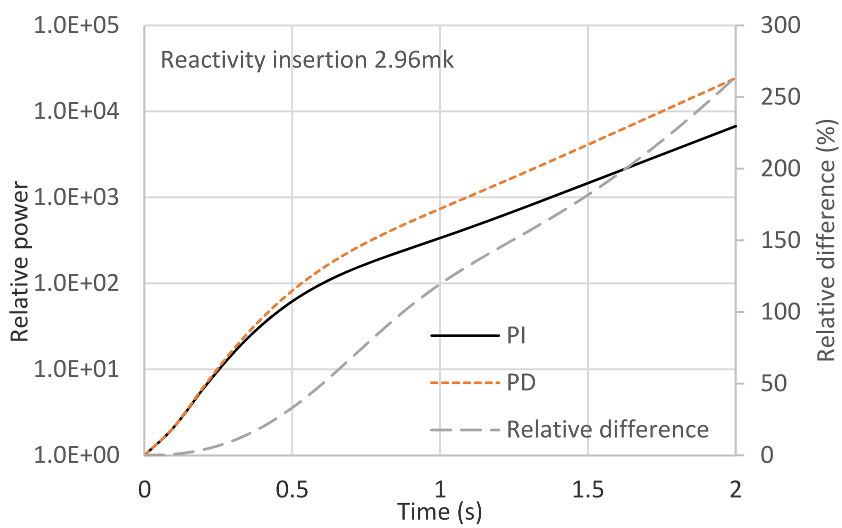

Figure 6 Relative core power as a function of time for the increased-reactivity scenario

3.3 Control-rod insertion scenario

To study the change in the effective delayed-neutron fractions caused by changes in the flux shape, a new transient is simulated, one induced by partial core voiding followed by insertion of the control rods.

The transient is initiated at 0.0s by partial voiding with enhanced reactivity insertion (2.96mk) in the centre region (10MWd/kg fuel). At 0.5s, control rods are inserted from the top in the voided region, at a speed of 5m/s. Control rods become fully inserted at 1.5s, when they reach the bottom of the core. The transient lasts 2.0s. The control-rod insertion is simulated by increasing the thermal absorption cross section in the region containing the rods by 10%.

Fig. 7 depicts the core power change during this control-rod insertion scenario. The core power peaks at 0.5s and starts dropping rapidly due to the insertion of the control rods. It is seen that the difference in the core relative power between the PD and the PI model reaches 37% after 0.5s and drops to 20% at the end of the transient.

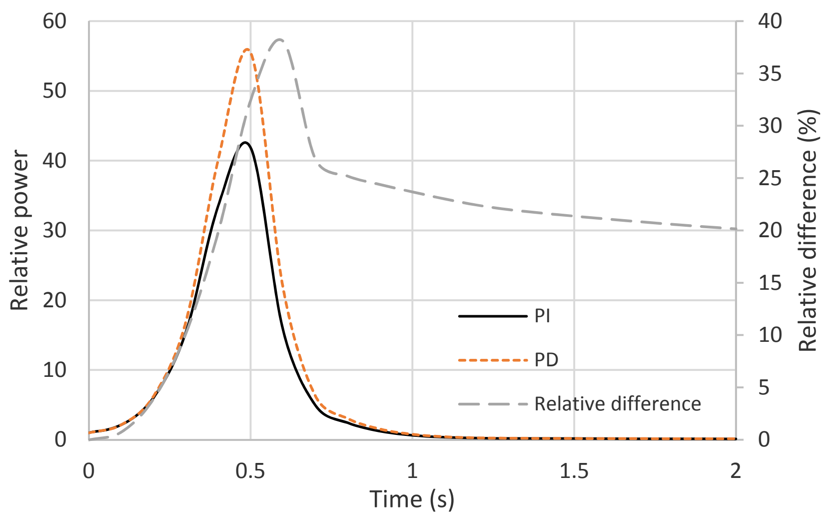

Figure 7 Power as a function of time in the control-rod insertion scenario.

The thermal flux shapes at 0.0s, 0.5s and 1.5s into the transient are shown in Fig. 8. It is seen that the partial voiding increases the flux slightly in the central region, while the insertion of the control rods causes a large dip in the flux shape. Nevertheless, the change in the core effective delayed-neutron fractions is less than 0.2% as shown in Table 2. This is because the core effective parameters are calculated as the ratio of bilinear functionals weighted by the steady-state adjoint flux as expressed in Eq. (4).

The thermal flux and adjoint shapes shown in Fig. 4 show that the low-burnup fuel region has a consistently higher weight than the high-burnup fuel region. As a result, the effective delayed-neutron fractions do not change too much during the control-rod insertion scenario, even though control-rod insertion causes a large change in the flux shape.

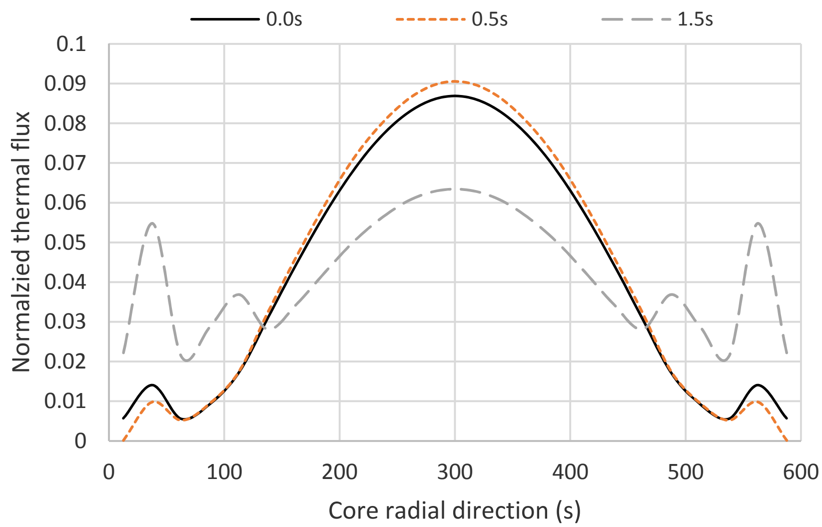

Figure 8 Thermal flux shape in the transient with control-rod insertion

Table 2 Effective delayed-neutron fractions in transient with control rods insertion.

Delayed-neutron group	0.0s	0.5s	1.5s
1	9.580E-05	9.582E-05	9.640E-05
2	7.526E-04	7.529E-04	7.538E-04
3	5.334E-04	5.339E-04	5.343E-04
4	1.151E-03	1.151E-03	1.153E-03
5	6.093E-04	6.094E-04	6.099E-04
6	2.041E-04	2.042E-04	2.044E-04
total	3.346E-03	3.347E-03	3.352E-03

4. Conclusion

The ability to model position-dependent delayed-neutron fractions was implemented in the IQS calculation of the diffusion code DONJON. Transient scenarios consisting of coolant partial voiding, enhanced reactivity insertion and control-rod insertion for a PT-SCWR core using different fuel loading patterns were simulated to test the functionality of the newly-implemented capability and to investigate the kinetic characteristics of the PT-SCWR. Accounting for the position dependence of the delayed-neutron fractions for a realistic positive reactivity insertion scenario induces an 11% difference in the core relative power at 2.0s. The closer the transient is to prompt criticality, the larger the difference in the core relative power between the PD and the PI model. Control-rod insertion causes a large change in the flux shape but almost no change in the delayed-neutron fractions. For the control-rod insertion scenario, only small differences are observed in the whole-core effective delayed-neutron fractions between the PD and the PI model, because the delayed-neutron fractions for different burnup fuel regions is merely 3%. The large flux shape change caused by the rod insertion does not cause major changes in the effective delayed-neutron fractions during the transient, because the weight of the low-burnup fuel region remains dominant and thus the whole-core effective delayed-neutron fractions remain close to the ones of the low-burnup region.

Future kinetics studies will have to be conducted for the Pressurized Heavy-water Reactor (PHWR), in which the delayed-neutron fractions have stronger dependency on fuel burnup.

5. Acknowledgement

Funding to the Canada Gen-IV National Program was provided by Natural Resources Canada through the Office of Energy Research and Development, Atomic Energy of Canada Limited, and Natural Sciences and Engineering Research Council of Canada.

The authors would like to thank Mr. Peter Schwanke for providing the initial DONJON PT-SCWR model.

6. References

[1] D. Rozon, "Nuclear Reactor Kinetics", Polytechnic International Press, Montreal, QC, Canada, 1998, pp. 263-286.

[2] K.O. Ott and R.J. Neuhold, "Nuclear Reactor Dynamics", Am. Nucl. Soc., 1985, pp. 294-299.

[3] B. Rouben, "Overview of Current RFSP-Code Capabilities for CANDU Core Analysis", Proceedings of the Annual General Meeting of the American Nuclear Society, Philadelphia, PA, 1995 June.

[4] E. Varin, A. Hebert, R. Roy and J. Koclas, "A User Guide for DONJON v. 3.01", Ecole Polytechnique de Montreal, 2005.

[5] M. Yetisir, M. Gaudet and D. Rhodes, "Development and Integration of Canadian SCWR Concept with Counter-Flow Fuel Assembly", "Development and Integration of Canadian SCWR Concept with Counter-Flow Fuel Assembly", Proceedings of the 6th International Symposium on Supercritical Water-Cooled Reactors, Shenzhen, Guangdong, China, 2013 March 3-7.

[6] G. Marleau, A. Hebert and R. Roy, "A User Guide for DRAGON, Release 3.05E", ", Institut de génie nucléaire, Département de génie mécanique, Ecole Polytechnique de Montréal, Montréal, Canada, 2007.

[7] F. Leszczynski, D. Lopez, Aldama and A. Trokov, "WIMS-D library update", IAEA, Vienna, Austria, 2007.

[8] P. Schwanke and E. Nichita, "Preliminary Space-Time Kinetics Simulation of A Coolant Voiding-induced Transient for A Supercritical Water Cooled Reactor with Re-Entrant Fuel Channels", Proceedings of 19th Pacific Basin Nuclear Conference, Vancouver, British Columbia, 2014, August 24-28.

[9] Q. Liu and E. Nichita "Position-Dependent Delayed-Neutron Fractions for IQS Calculations in the Diffusion Code DONJON and Application to PT-SCWR Reactors", Trans. Am. Nucl. Soc. 113, 2015.

[10] E. Nichita, "Kinetics Parameters of a Th-Pu Re-Entrant-Channel Pressure-Tube SCWR", Trans. Am. Nucl. Soc. 109, 2013.